Natural Resources for Human Health

eISSN: 2583-1194

Original Research

Received 22 May 2026
Revised 28 June 2026
Accepted 21 July 2026

Natural Resources for Human Health 2026, Vol. 6 (8s): 649–662

KEYWORDS:
Machine Learning, Transfer Learning, Chronic kidney disease, Optimization, CT Scans

FusionEffNet: An EfficientNet-Based Transfer Learning Model with Dual-Path Feature Fusion and AdamW Optimization for Multi-Class Kidney Disease Classification from CT Scans

Pulse Rajan[1], Nikhith Vasab[2], Pruthviraj Jitendra Pasee[3], Nirmal Keshari Swain[4], Deepika Davuluri[5], Vipul Mehra[6], Debabrata Swain[7*], Manish Kumar[8]*

[1]Department of Computer Science and Engineering, Pandit Deendayal Energy University, Gandhinagar, India, E-mail: Pulse.rajan22@gmail.com
[2]Microsoft Corp, Seattle, WA 98121, USA, E-mail: vasanikhith@gmail.com
[3]Department of Computer science and engineering, Vishwakarma Government Engineering College, Ahmedabad, India, E-mail: pruthvirajpasi676@gmail.com
[4]Department of Information Technology, Vardhaman College of Engineering, Telengana, India, swain.nirmal6@gmail.com, ORCID ID: 0000-0002-6845-5808
[5]Department of Chemistry, Michigan State University, Facility for Rare Isotope Beams, Department of Energy, East Lansing, MI 48823, USA, E-mail: deedavuluri@gmail.com
[6]GEICO, California, USA, E-mail: vmeh2392@gmail.com
[7*]Department of Computer Science and Engineering, Pandit Deendayal Energy University, Gandhinagar 382007, India, E-mail: debabrata.swain7@yahoo.com
ORCID iD: https://orcid.org/0000-0001-7775-3244
[8*]Department of Electronics and Communication Engineering, Pandit Deendayal Energy University, Gandhinagar 382007, India, E-mail: manishkumar087@gmail.com, ORCID iD: https://orcid.org/0000-0002-3003-9649
Corresponding author: Debabrata Swain, Manish Kumar

ABSTRACT: The detection of chronic disease is always a major challenge in health care sectors. Early and accurate detection can help in fast recovery of these types of diseases. Several renal diseases such as cysts, tumors and stones may come in this category and can save life by early detection. The modern computational methods like machine learning and deep learning with smart medical imaging techniques may assist in reliable diagnosis, enhancing early detection of kidney illnesses and reducing diagnostic errors in the healthcare industry. In this study, the combination of convolutional architecture and optimized transfer learning techniques can improve diagnostic accuracy of kidney related diseases. A large dataset of 20077 CT images is used in the study, and the result shows optimal accuracy related to multi class kidney diagnostic classes including cyst, tumor, stone, and normal using FusionEffNet. The result of the study will defenetly improve the diagnosis process and treatment process in healthcare sectors.

1. INTRODUCTION

Chronic kidney disease (CKD) is an illness where there is constant advancement of disability in kidney function over time. CKD is present in over 10% of the world's population, or around 800 million people. Incidence in India ranges geographically and is higher with more recent incidence figures ranging up to 17% in some areas. [1]. The increasing burden of CKD has been attributed to the meteoric rise in risk factors such as obesity, hypertension, diabetes, and other cardiovascular diseases [2]. Diabetes and hypertension together cause 40–60% of CKD cases in India [3]. The burden is also high due to the prevalence of these conditions, which is why CKD is common in the country. Early detection of kidney abnormalities is necessary to avoid delays in treatment and management [4]. Traditional methods, however, are dependent on the clinician's expertise and skill and hence are likely to be inconsistent with a risk of treatment delay. Providing it with the use of high-resolution imaging devices like CT scans along with deep learning algorithms can deliver diagnosis more swiftly and accurately. Deep learning algorithms like convolutional neural networks (CNN), have demonstrated dominant performance in image analysis to detect complex patterns in medical images. With these technologies, human error can be reduced to a minimum and early diagnosis can be possible [5].

Delayed or missed diagnosis of kidney disorders can lead to severe and often irreversible consequences on patient's health. Prompt diagnosis and early treatment are crucial in the treatment of kidney diseases. However, a significant proportion of cases remains undiagnosed or are diagnosed at a delayed period [6]. Thus, leading to poor clinical outcomes. Patients with late stages of CKD are more likely to "crash land" onto dialysis, which can cause the most disturbance to their daily lives, reduces their overall family income and harms physical as well as mental health. Moreover, delayed referral to nephrologists is associated with high early hospitalization and mortality [7, 8]. A study concluded that late-referred patients to nephrologists had greater mortality and high early hospitalization compared to the earlier-referred patients. Risks Associated with Misdiagnosis: Renal disease can remain undiagnosed, or diagnosed inaccurately, resulting in inappropriate treatment with dangerous consequences [9, 10]. For instance, incorrect diagnosis of kidney injury when the patient is dehydrated or vice versa has catastrophic interventions. Failure to treat dehydration in an emergency result in irreversible damage to kidneys, whereas over-rehydration in patients who have already suffered renal injury results in pulmonary edema because of fluid build-up in lungs [11, 12]. Further, CKD misstating can hinder the initiation of early intervention to slow disease progression and treat complications such as cardiovascular disease [13]. One study has found that stage 4 CKD can be correctly identified by primary care clinicians in only 63% of test cases through a high difference between correct and incorrect diagnosis. Psychosocial and Economic Impact: The progression of CKD to kidney failure involves substantial economic burdens on patients in the form of reduced incomes as well as expensive frequent treatment [14]. Caregivers also experience guilt, further making it difficult for the patients to psychologically adjust. Strong social support was found to reduce patient delays in seeking treatment, leading to healthy behaviours and coping styles [15].

To receive effective treatment for kidney abnormalities, it is necessary to have a timely and accurate diagnosis. Different clinical tests suggested by specialists for detection of kidney abnormalities are Serum Creatinine, Urinalysis, Kidney Ultrasound and Kidney Biopsy [16]. These diagnostic methods are often used in combination to provide a comprehensive evaluation of kidney health. Which facilitates accurate diagnosis and helps in providing appropriate treatment strategies [17]. Deep learning technology helps in early detection of disease based on medical images and clinical data. The Methode makes a complex network architecture-based relation among the images and data [18].

2. RELATED WORKS

This paper dealt with the application CNNs to detect kidney stones in CT scans. In this study they found GrayNet-pretrained CNNs were superior and its achieved 95% accuracy and an AUC of 0.954. The model was cross validated on 535 CT scans. The research tackled how deep learning, or CNN-based transfer learning, enhances the sensitivity and robustness of stone detection while focusing on kidney stones as a homogeneous class [19].

MSS U-Net, a high-performance multi-scale supervised deep learning network for renal and tumour segmentation from CT scans, was proposed in this paper. In contrast to widely used models, MSS U-Net improved segmentation accuracy with deep supervision and an improved loss function. The KiTS19 dataset, a well-established standard dataset for renal tumor segmentation, was used to test the model. It outperformed earlier segmentation approaches in terms of Dice coefficients of 0.805 for tumor and 0.969 for renal segmentation [20].

This study aimed to forecast early-stage CKD with the combination of deep learning and the Internet of Medical Things (IoMT). The proposed model used an adaptive hybridized deep CNN model that reduces feature complexity while achieving high classification accuracy. The system was developed for detecting CKD, where the process did not require constant human intervention. The model was evaluated against a large patient record database and categorized cases into two groups, which are CKD and healthy kidney. The results underlined the use of deep learning and IoMT based methods to transform kidney disease diagnosis through better efficiency [21].

Natural Resources for Human Health
eISSN: 2583-1194

In this research, it was tested whether radiomics and machine learning could be potential predictors of CKD. The authors retrospectively assessed CT scans from 50 abdominal radiation therapy treated patients and checked their kidney function 12 months later. The authors derived 140 radiomic features from the kidney images and compared six different machine learning models. Of these, the Random Forest classifier had the highest accuracy (94%) and was therefore the best model to predict kidney damage. The study divided cases into two classes patients with radiation-induced CKD and patients with normal kidney function. The results indicated that radiomics-based AI models could assist physicians in detecting patients at risk of kidney injury much earlier than current methods [22].

This paper introduced a deep learning system for the detection and classification of renal tumors based on a new database of 8,400 CT images. The authors tried three models, which are CNN-6, ResNet50, and VGG16. Of the three, the top performance was by CNN-6 (97%), followed by ResNet50 (96%) and CNN-4 (92%). The data were split 20% for testing and 80% for training to evaluate them fairly. The study focused on two groups— cancer and normal kidneys and highlighted the possibility of deep learning in reducing radiologists' workload through auto-detection of tumors [23].

This paper investigated three different deep-learning-based segmentation techniques for kidney and kidney stone detection from CT scans. Five different deep segmentation networks were tried and compared in terms of architecture and performance for three different 2D and 3D segmentation tasks. The models presented used semantic segmentation techniques, which yielded precise segmentations of the kidney. The open-source abdominal CT database was used for testing and training the dataset to enable benchmarking of segmentation performance [24].

This paper introduced MSKd_Net, a multi-head attention-based Swin Transformer model, for accurate classification of kidney pathologies from CT scans achieved F1-scores of 0.97 (cyst), 0.99 (normal), 0.98 (stone), and 0.90 (tumor). The paper has four major classes of renal diseases are cysts, stones, tumors and normal [25].

This paper suggested a deep learning based multi-class kidney detection model from computed tomography (CT) scans. Researchers created and annotated a dataset of 12,446 CT scans of four large classes kidney stones, cysts, tumors, and normal kidneys. The paper suggested a YOLOv8 based detection model, optimized for real-time clinical use. The overall performance of the model was evaluated with a global accuracy of 82.52%, precision of 85.76%, and recall of 75.28%. The paper demonstrated how AI based systems can help radiologists detect and classify kidney disease more effectively [26].

This review is a testimony to the amazing progress of AI based detection of kidney disease, and it shows the direction in which the science has been progressing over the decades. Early research was going on CNN-based detection and segmentation models, which were still the backbone of computer-assisted kidney abnormality detection [27]. However, recent research focused on multi class classification models and real-time AI based platforms, optimizing the efficiency of the diagnosis. The transformer-based models and YOLO models breakthrough in 2024 transformed real-time kidney disease detection to an even quicker, more precise, and highly reliable process for clinical application. Such technology may relieve radiologist workload, reduce diagnostic errors, and optimize early intervention, and hence improve patient outcome in nephrology and medical imaging [28]. The brief of the literature review are summarized in the table 1.

Table 1. Summary of the Literature review.

Ref. No	Author	Model	Hyperparameter Tuning	Preprocessing	Data Balancing	Limitations
19	Parakh et al., 2019	Cascaded CNNs, GrayNet-pretrained CNNs	Yes (different training methods)	Not specified	No	Focusing on kidney stones as a homogeneous class
20	Zhao et al., 2020	MSS U-Net	Not specified	Connected-component-based post-processing technique	No	Focus on two crucial classes: kidneys and kidney tumors

21	Chen et al., 2020	Adaptive hybridized deep CNN	Not specified	Not specified	No	Early-stage CKD prediction
22	Amiri et al., 2021	Random Forest classifier	Not specified	Radiomic feature extraction	No	Prediction of radiation-induced CKD
23	(Alzu'bi et al., 2022)	CNN-6, ResNet50, VGG16, CNN-4	Not specified	Data split (80% training, 20% testing)	No	Focus on two groups—cancer and normal kidneys
24	(Li et al., 2022)	Deep segmentation networks	Not specified	Not specified	No	Kidney and kidney stone detection
25	(Yan & Razmjooy, 2023)	Deep Belief Network (DBN)	Yes (optimized model)	Not specified	No	Detection of kidney stones
26	(Abdimurotovich & Cho, 2024)	Optimized YOLOv5	Yes (optimized using SE block)	Channel-wise recalibration	No	Real-time detection of kidney stones
27	(Sharen et al., 2024)	MSKd_Net: Multi-Head Attention-Based Swin Transformer	Not specified	Hierarchical learning	No	Classification of kidney pathologies
28	(Pande & Agarwal, 2024)	YOLOv8-based detection model	Yes (optimized for real-time clinical use)	Dataset creation and annotation	No	Multi-class kidney pathology detection

The comprehensive review of existing literature highlights significant advancements in the field of kidney abnormality detection utilizing deep learning and machine learning models. However, various research gaps remain unaddressed, which pave the way for further exploration and improvement.

The majority of studies target primarily the diagnosis of specific diseases such as kidney stones but not the multi-class classification of multiple types of kidney tumors. A complete, multi-class classification scheme is under-developed. While hybrid approaches have been utilized by some researchers to achieve better accuracy, they only operate as black boxes with limited interpretability options. Ensemble methods that use several architectures (CNN, ResNet, Transformer models) have not been properly explored either.

Although methods of data augmentation have been applied, imbalance of classes remains an issue. Existing research has not comprehensively exploited advanced methods of dataset augmentation. Experiments have infrequently compared head-to-head deep learning to conventional machine learning models (e.g., SVM, Random Forest) in a common experimental environment, limiting comprehensive understanding of model performance.

3. PROPOSED WORK

This study creates a deep learning framework that is reliable and effective for automatically identifying and classifying renal diseases into multiple classes from computed tomography (CT) scans. The suggested system uses convolutional neural networks' (CNNs') representational power and contemporary pretrained architectures' transfer-learning capabilities to reliably differentiate between cyst, tumor, stone, and normal renal conditions.

Natural Resources for Human Health
eISSN: 2583-1194

The traditional machine-learning models like Support Vector Machines (SVM) or K-Nearest Neighbors (KNN) are used manually to correlate the engineered features whereas CNN-based systems are capable of automatically learning from medical images and capturing variations that are essential for disease diagnosis.

3.1 Dataset Collection

This study used openly available dataset of four different types of CT kidney containing normal, cyst, tumor and stone collected from PACS (picture archiving and communication system) from diverse hospitals in Dhaka, and Bangladesh [29].

3.2 Data Preprocessing

3.2.1. Data Augmentation

Data augmentation techniques are used to represent the different classes of the dataset like cyst, tumor, and stone, especially minimizing the biasing of the model due to the uneven distribution of classes. To create realistic image variations while maintaining diagnostic features, augmentation operations such as random rotation, flipping, brightness enhancement, contrast adjustment, and Gaussian blur filtering were carried out using the torchvision library by increasing the sample size to 5000 images per class. It helps to balance the dataset. The class-wise augmented distribution is shown in Table 2 and the augmented images are shown in Figure 1.

Table 2. Sample Distribution.

	Cysts	Tumor	Stone	Normal
Before Augmentation	3709	2283	1377	5077
After Augmentation	5000	5000	5000	5077

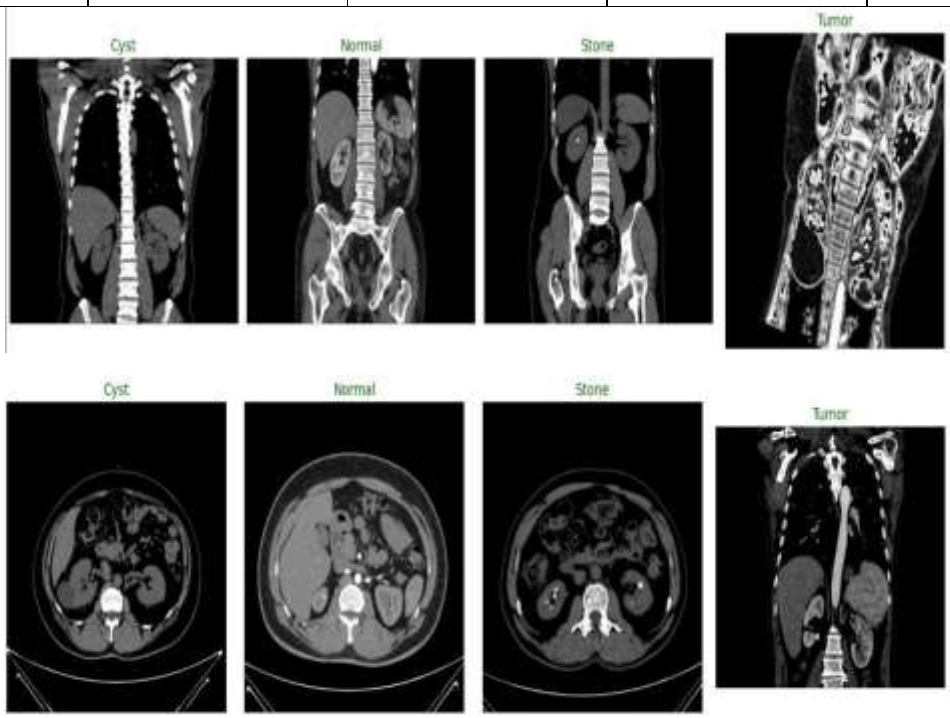

Fig. 1. Augmented samples.

3.2.2. Image Normalization and Rescaling

Several preprocessing techniques were carried out to enhance the input data quality before feeding the CT scan images into the CNN model. The pixel value normalization uses the transformation as shown in equation (1) to rescale pixel values from the original [0,255] range to a normalized [-1,1] scale. This was applied to each image to bring the intensity values to a common range [30].

$$I' = \frac{I}{127.5} - 1 \tag{1}$$

Where, I = original pixel value (0 to 255) and I'= normalized pixel value (mapped to -1 to +1)

This normalization guarantees that all input channels contribute consistently to gradient updates and improves convergence during training. In order to make it computationally efficient and preserve important anatomical details, all images were also uniformly rescaled to 192 × 192 pixels.

3.2.3. Image Filtering

As part of the preprocessing pipeline, Gaussian blur filtering was used to further increase the model's accuracy and reduce the excessive noise in the image. High-frequency fluctuations, which are caused by motion artifacts, scanner noise, or low-contrast textures were frequently found in the CT scans. Decreasing these fluctuations smoothen the image. The two-dimensional Gaussian function [31], which can be expressed mathematically as shown in equation (2).

$$G(x,y) = \frac{1}{2\pi\sigma^2} \cdot e^{-\frac{x^2+y^2}{2\sigma^2}} \tag{2}$$

Where, G(x,y) is the value of the Gaussian function, x and y are the horizontal and vertical distances from the origin and σ is the standard deviation.

CNN ignores small differences that have no bearing on classification accuracy using this method. Analysis is done on key structural patterns. Filtering techniques were frequently overlooked in earlier kidney CT classification studies. To increase precision and effectiveness, the suggested model incorporates Gaussian denoising. Generalization across CT scans acquired under various conditions is improved by this addition as shown in the Figure 2.

Fig. 2 Gaussian Blur Representation.

3.3 Training Phase

A dual-path architecture is used to extract features from image samples during training. The core feature extractor for its compound scaling technique is EfficientNetB0. High accuracy at low computational cost is achieved by balancing network depth, width, and resolution. EfficientNetB0 optimizes all three dimensions simultaneously, in contrast to conventional CNNs that scale each one independently. When real-time inference is needed and resources are scarce, medical imaging can benefit from this efficiency. EfficientNetB0 can capture hierarchical features at various scales thanks to the inverted residual blocks with squeeze and excitation mechanisms. Significant structural and subtle pathological changes are identified in the kidney CT images.

3.3.2 EfficientNet B0 as the Feature Extractor

Feature extraction is performed through a framework pretrained with a transfer learning approach based on the EfficientNetB0 architecture [32]. The method uses EfficientNetB0 as a frozen convolutional backbone to retain its hierarchical feature representation with minimal computation [33]. Unlike traditional CNNs, EfficientNetB0 applies compound scaling to balance depth, width, and resolution for higher accuracy. The model suits medical image analysis where small intensity differences hold diagnostic importance. Fine-grained texture patterns in CT images are effectively captured. Global Average Pooling is applied to the EfficientNet output feature maps to achieve global feature aggregation. The extracted features accurately represent high-level kidney structure semantics.

3.3.3 Dual-Path Fusion Strategy

By combining local fine details with global contextual information about the kidney, the suggested dual-path feature extraction system improves discriminative performance [34]. In the first path, spatial information is compressed into a compact global representation by Global Average Pooling, while normalization preserves steady gradient flow [35]. The pretrained EfficientNetB0 features are refined for CT-specific features in the second path using L2 regularization, ReLU activation, and additional convolutional layers with 1×1 and 3×3 kernels. Sensitivity to minor pathological areas, such as early lesions or slight structural alterations, is increased by this route [36]. A comprehensive feature vector that depicts both macro-level kidney structures and micro-level abnormalities is produced by combining the outputs of both paths. Figure 3 displays comprehensive model architecture.

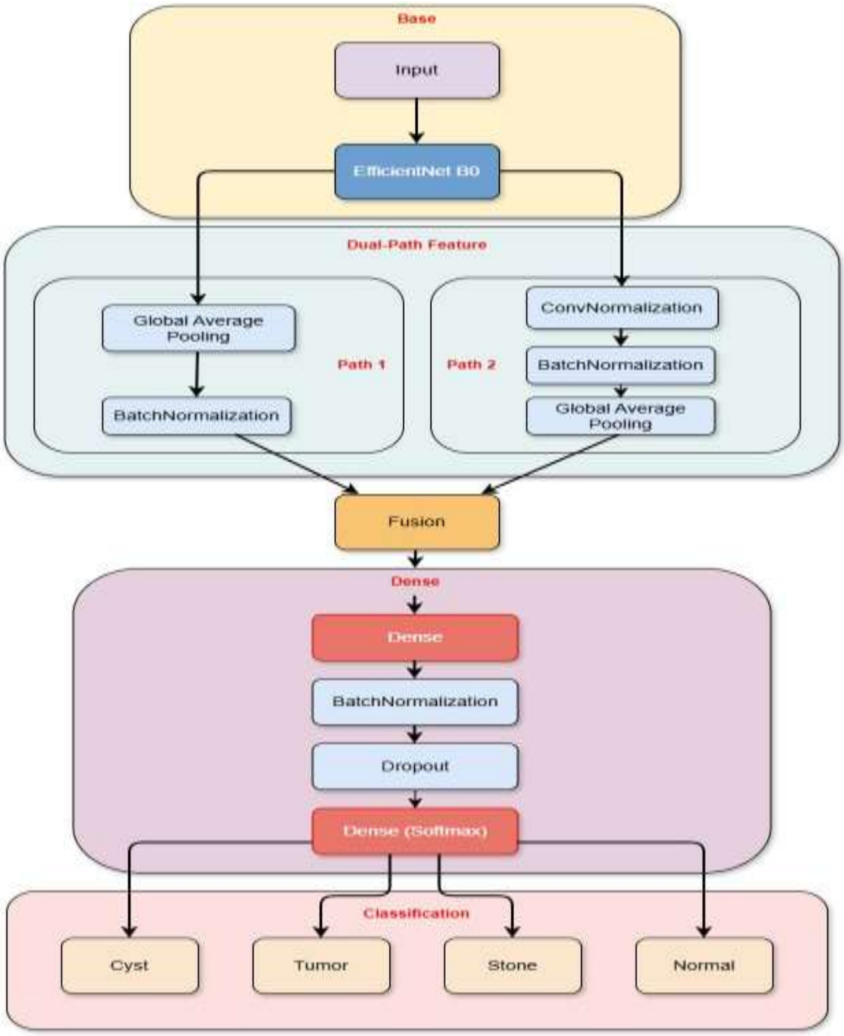

Fig. 3. CNN Model Architecture.

eISSN: 2583-1194

3.3.4 Model Training

A balanced dataset of 20,077 CT scan images from four distinct diagnostic classes cyst, tumor, stone, and normal was used to train the suggested architecture. The dataset was divided into 70% training and 30% testing, with 20% from the training data used for the validation. The AdamW optimizer was used for training, with an initial learning rate of 3×10^{-4} [37]. A custom "LearningRateScheduler" callback was employed to implement a staged warm up and exponential decay schedule to achieve gradual stability [38]. Every input image was fed in mini batches of 16 after being resized to 192 × 192 × 3 and normalized using EfficientNet preprocessing [39]. Data augmentation was also used to maximize generalization and reduce biasness between different classes. This included rotation (30°), width and height shifts (0.3), shear and zoom (0.2) and brightness variation (20 percent).

Accuracy and sparse categorical cross-entropy loss were used to compile the model network. While Dropout (0.5) and L2 regularization (1×10^{-2}) helped in reducing overfitting. Batch Normalization was incorporated throughout the model to stabilize gradient propagation. "ModelCheckpoint" callbacks were used during training to maintain both the final and best performing weights. To avoid out of memory errors during training on the NVIDIA Tesla P100 GPU, GPU memory growth was specifically controlled. Every epoch the model's performance was monitored on the validation set. The finished model is stored as "kidney_disease_model.h5" demonstrated stable convergence behavior with a test accuracy of over 98%. Reliable multi-class classification was confirmed by performance evaluation using precision, recall, F1-score, and confusion matrix analysis. Detailed CNN architecture is illustrated in Table 3. The total parameters are 4,556,903 in this study in which the trainable parameters are 503,876 and Non-trainable parameters are 4,053,027.

Table 3. Layered Structure CNN architecture.

Layer (type)	Output Shape	Param #	Connected to
input_layer_1 (InputLayer)	(None, 192, 192, 3)	0	-
efficientnetb0 (Functional)	(None, 6, 6, 1280)	4,049,571	input_layer_1
conv2d (Conv2D)	(None, 6, 6, 128)	163,968	efficientnetb0
batch_normalization (BatchNormalization)	(None, 6, 6, 128)	512	conv2d
conv2d_1 (Conv2D)	(None, 6, 6, 128)	147,584	batch_normalization
global_average_pooling2d (GlobalAveragePooling2D)	(None, 1280)	0	efficientnetb0
batch_normalization_1 (BatchNormalization)	(None, 6, 6, 128)	512	conv2d_1
batch_normalization_2 (BatchNormalization)	(None, 1280)	5,120	global_average_pooling2d
global_average_pooling2d_1 (GlobalAveragePooling2D)	(None, 128)	0	batch_normalization_1
concatenate (Concatenate)	(None, 1408)	0	batch_normalization_2, global_average_pooling2d_1
dropout (Dropout)	(None, 1408)	0	concatenate
dense (Dense)	(None, 128)	180,352	dropout
batch_normalization_3 (BatchNormalization)	(None, 128)	512	dense

dropout_1 (Dropout)	(None, 128)	0	batch_normalization_3
dense_1 (Dense)	(None, 64)	8,256	dropout_1
batch_normalization_4 (BatchNormalization)	(None, 64)	256	dense_1
dropout_2 (Dropout)	(None, 64)	0	batch_normalization_4
dense_2 (Dense)	(None, 4)	260	dropout_2

3.3.2.1 Loss Function

The Categorical Cross-Entropy loss was employed in this study which quantifies the difference between the model's predicted probability distribution $y = (y1, \dots, yC)$. The loss for a single sample is defined formally as shown in equation (3).

$$LCCE(y, p\hat{}) = -\sum_{i=1}^{C} y_i \; log(\hat{pi}). \tag{3}$$

where the ground-truth class is denoted by $yi \in \{0,1\}$ and the predicted probability for class i is denoted by $\hat{pi}$. Reducing this loss motivates the network to give the right class a high probability [40].

3.3.2.2 Regularization

To prevent overfitting and stabilize training, L2 regularization was employed. The model formed smoother decision boundaries and decreased reliance on noisy CT features as a result of penalizing large weight magnitudes. Through empirical testing, a weight-decay coefficient of 1×10^{-2} was chosen. While lower values resulted in slight overfitting, higher values slowed convergence. The application of L2 regularization to convolutional and dense layers enhanced generalization to previously unseen kidney CT images while maintaining balanced parameter growth. When combined with dropout and the AdamW optimizer, the method increased robustness in the classification of medical images [41].

3.3.2.3 Optimizer

The Adam optimizer's decoupled weight decay variant, AdamW, is used in this study because of its better generalization capabilities in deep neural networks. In contrast to the conventional Adam optimizer, which uses weight decay to indirectly apply L2 regularization through the gradient update, AdamW separates weight decay from the moment-based gradient updates [42]. Adam generally over-adapts to noisy gradients and tends to accumulate stale momentum, which leads to weaker generalization on unseen data and less than ideal convergence. In contrast, AdamW improves robustness in high-capacity feature extraction backbones such as EfficientNetB0 by directly penalizing large weights, thereby preventing unchecked weight growth. The AdamW parameter update at step t for each parameter θ is given by equation (4).

$$\theta_{t+1} = \theta_t - \alpha \left(\frac{\widehat{m_t}}{\sqrt{\widehat{v_t}} + \epsilon} + \lambda\theta_t \right) \tag{4}$$

where, m_t is 1st moment (momentum term), v_t is 2nd moment (variance term), $\widehat{m_t}$, $\widehat{v_t}$ are bias-corrected estimates, α is learning rate, λ is weight decay coefficient and ϵ is numerical stability constant

4. HYPERPARAMETERS

Using an NVIDIA Tesla P100 GPU for training and evaluation, the suggested renal disease classification model was developed in Python. Using heuristic methods, hyperparameter tuning was accomplished by testing various configurations and selecting the final values based on the highest validation accuracy and the most stable training behavior. Learning rate of 0.0003 found to yield the most stable training and validation accuracy. After evaluating multiple learning rates heuristically. Initial tests of larger batch sizes produced much slower convergence and increased GPU memory usage. Using batch sizes of 16 helped in making the model more computationally efficient and a more stable gradient update. After noticing that lower rates caused overfitting. Using, slightly larger probability such as 0.5 resulted in balanced regularization and increased model learning capacity.

5. RESULTS

The suggested CNN model underwent evaluation on a balanced dataset consisting of 20,077 CT scan images and was trained for 100 epochs employing the AdamW optimizer with categorical cross-entropy loss. In the Figure 4 and 5 has shown a gradual decrease in loss, and consistent enhancement in accuracy during Training and validation phase of the model, that ultimately reduces the possibility of overfitting. In the study, normalized confusion matrix appears excellent precision and recall for all four classes cyst, tumor, stone, and normal. Most misclassifications occur between cyst and tumor due to having analogous morphological characteristics. The model having 98% validation accuracy and precision, recall and F1-score 0.95 across the class.

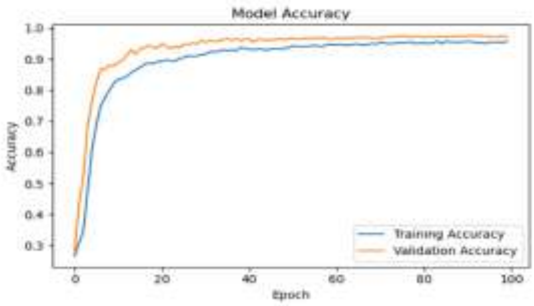

Fig 4. Accuracy Curve

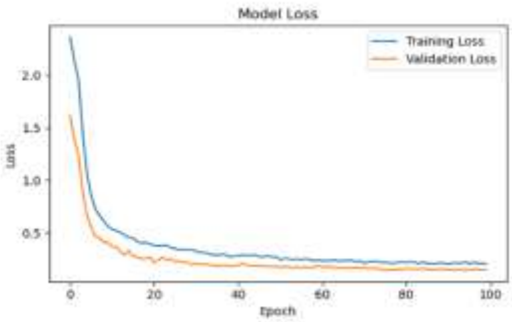

Fig 5. Loss Curve

5.1 Evaluation Metrics:

The TensorFlow Keras API was used to develop and test the model, which was trained on using a Nvidia Tesla 4 GPU and 16 GB of RAM. Several metrics, such as precision, recall, F1-score, and the confusion matrix, were used to assess the model's performance. These metrics offered a thorough evaluation of precision and practical efficacy. Table 5 displays the numerical results. The following is a list of the evaluation metrics that were employed.

Equation (5) defines precision as the percentage of correct positive predictions among all positive outputs.

$$\text{Precision} = \frac{TP}{TP+FP} \tag{5}$$

Equation (6) defines recall as the percentage of correctly identified positive cases among all actual positive cases. It shows how well all pertinent positive examples are found.

$$\text{Recall} = \frac{TP}{TP+FN} \tag{6}$$

Equation (7) defines the F1-Score, which has values between 0 and 1 and is the harmonic mean of precision and recall. It offers a fair assessment of classification accuracy as well as the capacity to reduce the number of missed positive cases.

$$\text{F1-score} = 2 * \frac{1}{\frac{1}{Precision}+\frac{1}{Recall}} \tag{7}$$

Table 4. Values of different evaluation metrics.

	Precision	Recall	F-1 score	Support
Cyst	0.97	0.99	0.98	1478
Normal	0.99	0.98	0.99	1557
Stone	0.97	0.96	0.96	1484
Tumor	0.97	0.97	0.97	1505

eISSN: 2583-1194

Confusion Matrix This is an N × N table, where N is the number of classes, or categories, the model is trying to predict. It can be seen in Figure 6. Four key terms to consider are True Positives (TP): Where the model said Yes and it was indeed Yes. True Negatives (TN): Where the model said No and it was in fact No. False Positives (FP): Where the model said Yes but it was No. False Negatives (FN): Where the model said No and it was Yes.

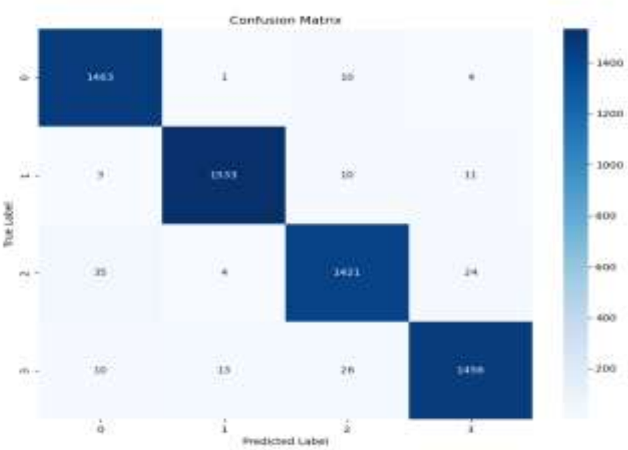

Fig. 6. Confusion Matrix.

6. COMPARATIVE ANALYSIS:

In general, models like MSKd_Net and transfer learning techniques like VGG16 and ResNet50 rely heavily on massive pre-existing datasets and complex initialization. This reduces the bias of the datasets produce due to irrelevant datasets like ImageNet. About 15.6 million parameters are used in this study with optimal feature extraction capacity in reduced processing power. The result shows fast convergence and higher validation accuracy compared to standard Adam optimizer without weight decay. In table 6, the detailed comparison of all the different models is listed below. The reason behind the superior performance of the proposed model lies with the dual path fusion architectural design of the model. The architecture obtained the global spatial features using the average pooling layer with the inclusion of an extra convolution operation. This combination of layers helped to capture the robust features before the classification decision. The Gaussian blur filter eliminates the high frequency noise from the image sample to make it suitable for clinical usecase solutions. During training, AdamW improves optimization by decoupling weight decay from the gradient update, which can provide better regularization and reduce overfitting compared with conventional Adam, while the learning-rate scheduler progressively adjusts the learning rate, allowing faster learning during the initial stages and more stable fine-tuning near convergence.

Table 5. Comparison of different parameters used in different studies.

Ref. No.	**Model Used**	**Accuracy**
19	CNN	95
20	U-Net	96
21	Adaptive Hybridized Deep CNN	97
22	Random Forest	94
23	VGG16 and Restnet50	97
24	DenseAUXNet201	90
25	Deep Belief Network	97
26	YOLO	81
27	MSKd_Net Swin Transformer	90
28	YOLOv8	82
FusionEffNet (Proposed Model)		98

7. CONCLUSION

In this work for categorizing different types of kidney disease condition, a custom neural network-based framework is used. The CT scan images are used for diagnosis of normal, cyst, tumor, and stone classes. The main intension behind the use of CT scan image in this research is its high reliability for medical use cases. The sample count is enhanced using augmentation techniques for enhancing the model performance. Gaussian filtering image rescaling and normalization techniques are performed during preprocessing to improve the efficiency of the model. The model performance is evaluated using accuracy, precision, recall and F-1 score. The important hyperparameter of the model is tuned using heuristic Methode to get the optimum performance of the model. The diagnosis accuracy shown by the proposed model is 98 %, which is better than all the referred literature. This promising performance of the model has proved its real time implication and reliable detection of the kidney abnormalities. This will speed up diagnosis processes and clinical decision making in the health care sector.

Declaration

The views and opinions expressed in this research paper are those of Vipul Mehra only and do not necessarily reflect the views, opinions, or official positions of GEICO. This paper was prepared by Vipul Mehra in an individual capacity. Nothing contained herein should be construed as an official statement or position of GEICO.

REFERENCES

[1] Khan, A., Das, R., & Parameshwara, M. C. (2022). Detection of kidney stone using digital image processing: a holistic approach. Engineering Research Express, 4(3), 035040.

[2] Kovesdy, C.P., 2022. Epidemiology of chronic kidney disease: an update 2022. Kidney international supplements, 12(1), pp.7-11.

[3] Varughese, S. and Abraham, G., 2018. Chronic kidney disease in India: a clarion call for change. Clinical Journal of the American Society of Nephrology, 13(5), pp.802-804.

[4] Shrestha, N., Gautam, S., Mishra, S.R., Virani, S.S. and Dhungana, R.R., 2021. Burden of chronic kidney disease in the general population and high-risk groups in South Asia: A systematic review and meta-analysis. PLoS One, 16(10), p.e0258494.

[5] Varma, P.P., 2015. Prevalence of chronic kidney disease in India-Where are we heading? Indian journal of nephrology, 25(3), p.133.

[6] Zheng, J., Xue, B.W., Guo, A.H., Feng, S.Y., Gao, R., Wu, S.Y., Liu, R. and Zhai, L.J., 2023. Patient delay in chronic kidney disease: a qualitative study. Medicine, 102(48), p.e36428.

[7] Sharma, K., Uddin, Z., Wadal, A. and Gupta, D., 2025. Hybrid Deep Learning Framework for Classification of Kidney CT Images: Diagnosis of Stones, Cysts, and Tumors. arXiv preprint arXiv:2502.04367.

[8] Farooq, M.S. and Tariq, A., 2024. A Deep Learning Architectures for Kidney Disease Classification. arXiv preprint arXiv:2403.15895.

[9] Zhang, M., Ye, Z., Yuan, E., Lv, X., Zhang, Y., Tan, Y., Xia, C., Tang, J., Huang, J. and Li, Z., 2024. Imaging-based deep learning in kidney diseases: recent progress and future prospects. Insights into imaging, 15(1), p.50.

[10] Singh, V., Asari, V.K. and Rajasekaran, R., 2022. A deep neural network for early detection and prediction of chronic kidney disease. Diagnostics, 12(1), p.116.

[11] Zhao, X., Gu, X., Meng, L., Chen, Y., Zhao, Q., Cheng, S., Zhang, W., Cheng, T., Wang, C., Shi, Z. and Jiao, S., 2024. Screening chronic kidney disease through deep learning utilizing ultra-wide-field fundus images. NPJ Digital Medicine, 7(1), p.275.

[12] Zhang, M., Ye, Z. and Yuan, E., Imaging-based deep learning in kidney diseases: recent progress and future prospects. Insights Imaging. 2024; 15: 50 [online]

[13] Arifuzzaman, M., Ahmed, I., Chowdhury, M.J.U., Sakib, S., Rahman, M.S., Hossain, M.E. and Absar, S., 2024. A Novel Ensemble-Based Deep Learning Model with Explainable AI for Accurate Kidney Disease Diagnosis. arXiv preprint arXiv:2412.09472.

[14] Aggarwal, R., Sounderajah, V., Martin, G., Ting, D.S., Karthikesalingam, A., King, D., Ashrafian, H. and Darzi, A., 2021. Diagnostic accuracy of deep learning in medical imaging: a systematic review and meta-analysis. NPJ digital medicine, 4(1), p.65.

[15] Miotto, R., Wang, F., Wang, S., Jiang, X. and Dudley, J.T., 2018. Deep learning for healthcare: review, opportunities and challenges. Briefings in bioinformatics, 19(6), pp.1236-1246.
[16] Thakur, G.K., Thakur, A., Kulkarni, S., Khan, N. and Khan, S., 2024. Deep learning approaches for medical image analysis and diagnosis. Cureus, 16(5).
[17] Xu, Z., Li, J., Yao, Q., Li, H., Zhao, M. and Zhou, S.K., 2024. Addressing fairness issues in deep learning-based medical image analysis: a systematic review. npj Digital Medicine, 7(1), p.286.
[18] Javed, H., El-Sappagh, S. and Abuhmed, T., 2024. Robustness in deep learning models for medical diagnostics: security and adversarial challenges towards robust AI applications. Artificial Intelligence Review, 58(1), p.12.
[19] Parakh, A., Lee, H., Lee, J.H., Eisner, B.H., Sahani, D.V. and Do, S., 2019. Urinary stone detection on CT images using deep convolutional neural networks: evaluation of model performance and generalization. Radiology: Artificial Intelligence, 1(4), p.e180066.
[20] Zhao, W., Jiang, D., Queralta, J.P. and Westerlund, T., 2020. MSS U-Net: 3D segmentation of kidneys and tumors from CT images with a multi-scale supervised U-Net. Informatics in Medicine Unlocked, 19, p.100357.
[21] Chen, G., Ding, C., Li, Y., Hu, X., Li, X., Ren, L., Ding, X., Tian, P. and Xue, W., 2020. Prediction of chronic kidney disease using adaptive hybridized deep convolutional neural network on the internet of medical things platform. IEEE Access, 8, pp.100497-100508.
[22] Amiri, S., Akbarabadi, M., Abdolali, F., Nikoofar, A., Esfahani, A.J. and Cheraghi, S., 2021. Radiomics analysis on CT images for prediction of radiation-induced kidney damage by machine learning models. Computers in Biology and Medicine, 133, p.104409.
[23] Alzu'bi, D., Abdullah, M., Hmeidi, I., AlAzab, R., Gharaibeh, M., El-Heis, M., Almotairi, K.H., Forestiero, A., Hussein, A.M. and Abualigah, L., 2022. Kidney tumor detection and classification based on deep learning approaches: a new dataset in CT scans. Journal of Healthcare Engineering, 2022(1), p.3861161.
[24] Li, D., Xiao, C., Liu, Y., Chen, Z., Hassan, H., Su, L., Liu, J., Li, H., Xie, W., Zhong, W. and Huang, B., 2022. Deep segmentation networks for segmenting kidneys and detecting kidney stones in unenhanced abdominal CT images. Diagnostics, 12(8), p.1788.
[25] Yan, C. and Razmjooy, N., 2023. Kidney stone detection using an optimized Deep Believe network by fractional coronavirus herd immunity optimizer. Biomedical Signal Processing and Control, 86, p.104951.
[26] Abdimurotovich, K.A. and Cho, Y.I., 2024. Optimized YOLOv5 architecture for superior kidney stone detection in CT scans. Electronics, 13(22), p.4418.
[27] Sharen, H., Narendra, M. and Anbarasi, L.J., 2024. MSKd_Net: Multi-Head Attention-Based Swin Transformer for Kidney Diseases Classification. IEEE Access.
[28] Pande, S.D. and Agarwal, R., 2024. Multi-class kidney abnormalities detecting novel system through computed tomography. IEEE Access, 12, pp.21147-21155.
[29] CT KIDNEY DATASET: Normal-Cyst-Tumor and Stone. (2021c, November 1). Kaggle. https://www.kaggle.com/datasets/nazmul0087/ct-kidney-dataset-normal-cyst-tumor-and-stone
[30] D. Swain, M. Kumar, N. Jain and C. Devnani, "Prediction of Bushfire Area Using Machine Learning Techniques," 2023 7th International Conference on Computing, Communication, Control and Automation (ICCUBEA), Pune, India, 2023, pp. 1-7.
[31] Tan, M. & Le, Q. V. (2019). EfficientNet: Rethinking Model Scaling for Convolutional Neural Networks (cite arxiv:1905.11946Comment: Published in ICML 2019).
[32] Zhang, Z., Yu, L., Liang, X., Zhao, W., & Xing, L. (2021, September). TransCT: dual-path transformer for low dose computed tomography. In International Conference on Medical Image Computing and Computer-Assisted Intervention (pp. 55-64). Cham: Springer International Publishing.
[33] Swain, D., Patel, S., Panchal, P., Singh, D. P., Mohanty, M., Swain, N. K., ... & MADHAVI, B. (2025). HydroBoost Hybrid Model: A Novel SARIMAX–GBM Residual Learning Approach for Rainfall Spike Prediction.
[34] Tan, M., & Le, Q. (2019, May). Efficientnet: Rethinking model scaling for convolutional neural networks. In International conference on machine learning (pp. 6105-6114). PMLR.
[35] Bridle, J. (1989). Training stochastic model recognition algorithms as networks can lead to maximum mutual information estimation of parameters. Advances in neural information processing systems, 2.

[36] Smith, L. N. (2017, March). Cyclical learning rates for training neural networks. In 2017 IEEE winter conference on applications of computer vision (WACV) (pp. 464-472). IEEE.
[37] D. Swain, M. Kumar, N. Jain and C. Devnani, "Prediction of Bushfire Area Using Machine Learning Techniques," 2023 7th International Conference On Computing, Communication, Control and Automation (ICCUBEA), Pune, India, 2023, pp. 1-7.
[38] Srivastava, N., Hinton, G., Krizhevsky, A., Sutskever, I., & Salakhutdinov, R. (2014). Dropout: a simple way to prevent neural networks from overfitting. The journal of machine learning research, 15(1), 1929-1958.
[39] Deshmukh, O., Swain, N. K., Panda, T., Swain, D., Mehra, V., & Kumar, M. (2025, November). Machine Learning for Stroke Detection: Performance Evaluation of Random Forest and XGBoost Classifiers. In 2025 IEEE 3rd International Symposium on Sustainable Energy, Signal Processing and Cybersecurity (pp. 1-4). IEEE.
[40] Mahmud, S., Abbas, T.O., Mushtak, A., Prithula, J. and Chowdhury, M.E., 2023. Kidney cancer diagnosis and surgery selection by machine learning from CT scans combined with clinical metadata. Cancers, 15(12), p.3189.
[41] Patro, K.K., Allam, J.P., Neelapu, B.C., Tadeusiewicz, R., Acharya, U.R., Hammad, M., Yildirim, O. and Pławiak, P., 2023. Application of Kronecker convolutions in deep learning technique for automated detection of kidney stones with coronal CT images. Information Sciences, 640, p.119005.
[42] Asif, S., Zheng, X. and Zhu, Y., 2024. An optimized fusion of deep learning models for kidney stone detection from CT images. Journal of King Saud University-Computer and Information Sciences, 36(7), p.102130.